#2227

Pan-cancer shedding patterns of tumor circulating cell-free DNA

Fábio Navarro[1], Simo Zhang[1], Mengyao Tan[1], Charles Abbott[1], Josette Northcott[1], John Lyle[1], Gabor Bartha[1], Jason Harris[1], John West[1], Richard Chen[1], Sean Michael Boyle[1]
[1]Personalis, Inc., Menlo Park, CA;

Contact:
Fabio.Navarro@personalis.com
Sean.Boyle@personalis.com

I. Background

Tumor circulating cell-free DNA (ctDNA) comprises DNA molecules cast from tumors that reach and circulate in a patient's bloodstream. Given its non-invasive nature, the liquid biopsy of ctDNA has remarkable potential for diagnosis, prognosis, disease progression tracking, and treatment monitoring. Nonetheless, little is known about which tumor features yield a higher representation of ctDNA in blood or even which regions in the tumor genome are more inclined to shed and thus be observed as ctDNA.

II. Augmented exome capture with ImmunoID NeXT

Typically, studies of ctDNA have focused on a limited and well-established set of genes and recurrent variants. However, these limited gene panels may not capture the breadth of genetic alterations that reflect tumor biology. Their limited footprint hinders a comprehensive understanding of tumor heterogeneity, resistance mechanisms, and DNA shedding patterns. To address these limitations, we developed a whole-exome scale cfDNA platform, NeXT Liquid Biopsy™, that enables sensitive detection and tracking of mutations in over twenty thousand genes from plasma samples.

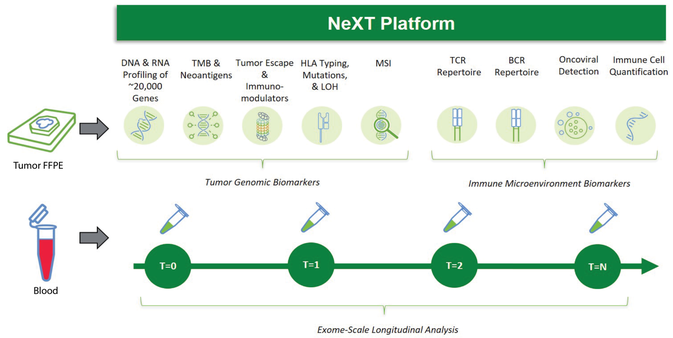

To investigate the tumor DNA shedding patterns, we sequenced tumor, normal, and plasma from 69 patients at different tumor stages and indications. Namely, we characterized 14 Gastrointestinal tumor patients, 14 Head & Neck, 12 Breast, 9 Lung, 6 Prostate, 5 Melanoma, 5 Colorectal, 3 Ovary, and one Uterus. Collectively, we uniformly sequenced, processed, and consolidated the somatic variants of over 122 liquid biopsies samples from 69 patients. We also characterized solid tumors in terms of their transcriptome, MSI, immune microenvironment, and neoantigens.

III. Detecting somatic variants from Liquid Biopsies

A. Variants detected in LB

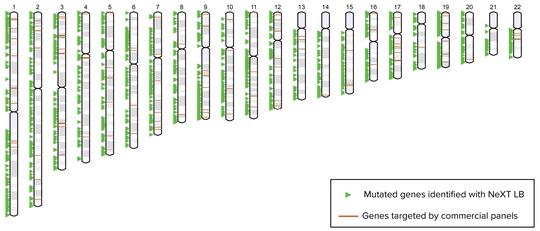

B. Landscape of variants AF

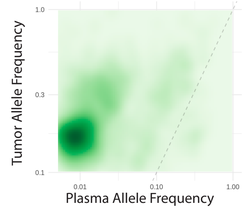

Using patients' cfDNA, we monitor tumor mutations scattered across 2,339 genes. These include canonical variants in highly penetrant genes and actionable targets such as TP53, APC, BRAF, EGFR, RET, and HRAS. Tracking such variants in plasma allows characterization and tracking tumor progression over time. Moreover, we accurately detect thousands of somatic variants exclusive to one patient (and missed by targeted strategies) and support a granular and longitudinal tumor characterization.

We then compare the allele fraction of somatic mutations detected in both tumor (AF>=10%) and liquid biopsies (AF>=0.5%). As expected, we observed a lessening in allele fraction in plasma samples, likely due to non-tumor circulating DNA. Since non-tumoral cfDNA is a significant plasma component, we needed to develop a new strategy to estimate the portion of ctDNA considering the healthy background.

IV. Estimating tumor shedding ratio compared to healthy LB

To increase understanding of the shedding signal generated by non-tumoral cfDNA, we sequenced and characterized 20 plasma samples from healthy individuals. Since these patients did not present any observable tumors, we used them as a cohort to: I. establish the expected shedding from non-tumoral DNA; and II. to contrast against ctDNA deriving from patients with tumors. As observed in previous works, the DNA fragments of healthy individuals' liquid biopsies tend to have longer fragments than DNA fragments of patients with tumors. To assess the tumor DNA shedding rate in liquid biopsies, we divided the genome into 100 nucleotide windows in length and calculated the mononucleosomal and sub-mononucleosomal coverage in each window. Using a model similar to differential expression, we calculate the enrichment or depletion of sequences for each window in the genome. Estimating the dispersion within each genomic window allows us to estimate the genome's windows with significant enrichment or depletion of cfDNA.

A. Distribution of fragment length of liquid biopsies from healthy individuals

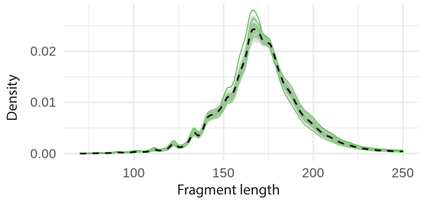

B. Differential shed regions model

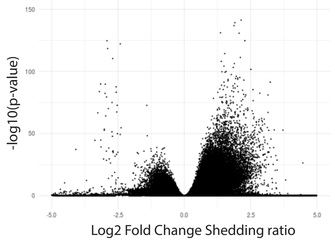

V. Dilution of normal and tumor cell-line pair as controls

We developed a cell media system to reproduce tumor DNA shedding at scale. Our cell media system allows us to control the fraction of DNA shed in the system. We diluted tumor DNA from HCC1143 at 5%, 10%, 15%, and 20% for this experiment. Our method replicated DNA fragments similar to those observed in the literature.

We then computed the differentially shed regions between healthy liquid biopsies and cell media dilutions. As expected, we observed that a significant increase in tumor DNA shedding regions correlating with tumor DNA dilution (p-value < 2.2e-16). Finally, we evaluated the genome-wide tumor DNA shedding patterns. We calculate the shedding delta the baseline dilution by subtracting the shedding estimates from the 5% dilution. Interestingly, we highlight an amplification on chromosome 19 (12 copies) that boosts the tumor DNA shedding signal—suggesting that amplified regions might have a higher representation in cfDNA.

A. Genome-wide shedding ratio (HCC1143)

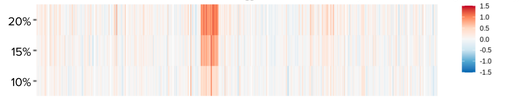

B. Highly amplified HCC1143 locus

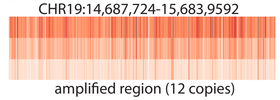

VI. Global patterns of tumor DNA shedding

We then applied our differential shedding strategy to the whole cohort of 122 plasma samples. First, we integrated external chromatin accessibility (ATAC-seq) data to investigate possible associations between chromatin state and tumor DNA shedding. We found DNA shed from tumors tends to be depleted in open chromatin regions—suggesting that the nucleosome-free regions might have a significantly weaker representation in liquid biopsies. Interestingly, we did not find a sharp association between gene expression level and over or under-representation of ctDNA (data not shown).

Nonetheless, when we applied our strategy to patients with longitudinal plasma collection, we were able to identify anecdotal examples of the increment and reduction of ctDNA in patients, respectively, non-responders and responders to immunotherapy.

A. Higher shedding is correlated with compacted chromatin

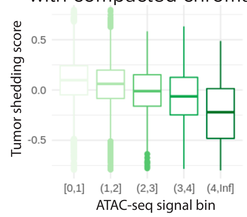

B. Genome-wide shedding ratio (Head&Neck - Non-responder)

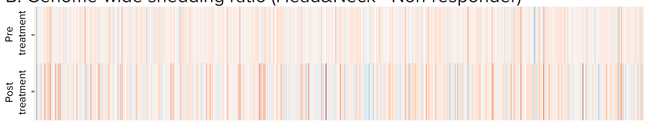

C. Genome-wide shedding ratio (Head&Neck - Responder)

VIII. Conclusion

We have developed a whole-exome scale technology, NeXT Liquid Biopsy, that enables sensitive monitoring and detection of somatic SNVs from cfDNA. The NeXT LB platform generates a much broader view of the tumor mutational landscape from the plasma than typical targeted liquid biopsy platforms. The platform enables broader monitoring of changes in response to cancer therapy, acquired drug resistance mechanisms, and intra- and inter-tumor heterogeneity. Using NeXT LB as a scaffold, we also were able to explore approaches to estimate granular tumor DNA shedding in liquid biopsies. With this strategy, we able to identify associations between tumor DNA shedding and chromatin accessibility. We were also able to identify distinct global patterns in tumor DNA shedding from responders and non-responders. Nonetheless, further investigations are required to generalize our findings in a larger and more heterogeneous cohort.

Personalis®